Impact Damping Analysis of Packaging Materials Using Static Compression Tests

Ding Lou

Hongwen School Shanghai Campus, Shanghai, China
Email: riane.lou@hongwenstudent.com (D.L.)
Manuscript received January 6, 2025; accepted May 5, 2025; published September 28, 2025.

***Abstract*—This study explores the damping characteristics of packaging fillers using static compression experiments. A custom-designed test rig was employed to analyze EPE pearl cotton under varying sample conditions and parameters. Experimental data were used to propose a modified damping model that better fits foam materials, reducing errors compared to the Hertz model. The study highlights the influence of thickness and compression speed on damping, while density and diameter showed minimal impact. Further validation through impact testing is required, and future work will explore alternative materials such as air bags and particulate fillers.**

***Keywords*—damping characteristics, packaging materials, static compression, EPE foam, energy dissipation**

I. Introduction

The rapid growth of e-commerce and logistics has intensified the demand for robust packaging solutions capable of withstanding the challenges of transportation. Express parcels are often exposed to impacts and vibrations, necessitating the use of packaging materials with sufficient impact resistance. To ensure the safety of packaged items while minimizing material usage, the impact resistance of various materials must be quantitatively evaluated. Such assessments are considered foundational for the establishment of scientifically informed packaging standards.

Damping characteristics, defined as a material's ability to dissipate energy under external forces, are regarded as a critical parameter for evaluating impact resistance. Traditional research in this domain has frequently been conducted through the combination of experimental measurements and theoretical modeling. For instance, a single-degree-of-freedom model was employed by Feng *et al.* [1] to determine the damping coefficient of foam materials by applying controlled vibrations and measuring transmission coefficients. This method is considered a classical approach to damping assessment.

An impact methodology was utilized by Ge and Rice [2] to obtain the force-displacement response of foam materials. Their approach was based on the seismic structural impact model proposed by Jankowski [3], which has been effectively applied in the analysis of nonlinear damping behavior in foam materials. Additionally, PU and EVA foams were studied by Ramirez and Gupta [4] using both impact and quasi-static compression methods to simulate high and low strain rate conditions, respectively. Although energy loss data were obtained in these scenarios, the findings were not extended to calculate damping coefficients.

Although significant contributions have been made by these methodologies to academic understanding, the reliance on specialized and costly experimental equipment has limited their accessibility for broader industrial applications. To address this limitation, a novel, simplified approach is proposed in this study, based on static compression experiments. Through the analysis of force-displacement graphs, energy loss values are derived, which are then converted into damping coefficients. This method is intended to provide a cost-effective and user-friendly solution, expanding the potential for industrial adoption and contributing to the development of practical packaging standards.

To achieve these objectives, a specialized experimental device was designed to measure force-displacement relationships. By establishing these advancements, a robust foundation has been provided for the development of new packaging standards, aimed at improving safety and efficiency in the logistics sector.

II. A Nonlinear Model of Damping

The Hertz model of damping is nonlinear and derived from the Hertz contact force model, which describes the force when a sphere contacts an infinitely large, rigid plane [5]:

$$F = \frac{4E}{3(1-\mu^2)}\sqrt{R}\cdot x^{\frac{3}{2}} \quad (1)$$

Here, E is the Young's modulus of the material, μ is the Poisson ratio, R is the radius of the sphere, and x is the depth of indentation. Since contact occurs between the mass and the foam when a heavy object falls, the contact force model can also describe the interaction between the object and the foam. According to this equation, the force is proportional to the 3/2 power of the displacement. The equivalent stiffness, k', of the material varies with displacement and is expressed as:

$$\mathrm{k'(x)} = \mathrm{kx}^{\frac{1}{2}} \quad (2)$$

During compression, the interaction force includes contributions from both elastic and damping effects. The force equation is written as [2]:

$$F = -kx^{\frac{3}{2}} - c(x)\dot{x} \quad (3)$$

where $c(x)$ is the displacement-dependent damping coefficient. However, during the rebound phase, damping effects are often negligible, and the force reduces to:

$$F = -kx^{\frac{3}{2}} \quad (4)$$

The corresponding equations of motion for the two phases are:

Compression:

$$\mathrm{m\ddot{x} + c(x)\dot{x} + kx^{\frac{3}{2}} = 0(\dot{x} > 0, 0 < x < x_{max})} \quad (5)$$

Rebound:

$$m\ddot{x} + kx^{\frac{3}{2}} = 0(\dot{x} < 0, 0 < x < x_{max}) \quad (6)$$

To analyze the dynamics further, we introduce the displacement-dependent natural frequency ω_n defined as,

$$\omega_n(x) = \sqrt{\frac{k\sqrt{x}}{m}} \quad (7)$$

Using this, the equations of motion can be rewritten in terms of the damping ratio ζ,

$$\ddot{x} + 2\zeta\,\omega_n(x)\dot{x} + \omega_n(x)^2\,x = 0 \quad (8)$$

The damping ratio ζ is calculated as:

$$\zeta = \frac{c(x)}{2\sqrt{mk\sqrt{x}}} \quad (9)$$

The energy dissipated during impact is the difference between the initial and rebound kinetic energies:

$$\Delta U = \frac{1}{2}mv_i^2 - \frac{1}{2}mv_r^2 = \frac{1}{2}mv_i^2(1 - C_r^2) \quad (10)$$

here, v_i is the impact velocity, v_r is the rebound velocity, and , the coefficient of restitution C_r , is defined as:

$$C_r = \frac{v_r}{v_i} \quad (11)$$

The energy input during loading is given by:

$$U_{load} = \frac{1}{2}mv_i^2 \quad (12)$$

Thus, the energy loss factor η becomes:

$$\eta = \frac{\Delta U}{U_{load}} = \frac{\frac{1}{2}mv_i^2(1-C_r^2)}{\frac{1}{2}mv_i^2} = 1 - C_r^2 \quad (13)$$

The dissipated energy can also be expressed as the work done against damping forces:

$$\Delta U = \int_0^{x_{max}} c(x)\dot{x}\cdot dx = \int_0^{x_{max}} 2\zeta\sqrt{mk\sqrt{x}}\dot{x}\cdot dx \quad (14)$$

Substituting this into the energy balance equation yields:

$$\frac{1}{2}mv_i^2(1 - C_r^2) = \int_0^{x_{max}} 2\zeta\sqrt{mk\sqrt{x}}\dot{x}\cdot dx \quad (15)$$

To solve the integral on the right-hand side of Eq. (15), it is necessary to express the velocity $\dot{x}$ as a function of the displacement x. An approximate expression for velocity $\dot{x}$ is constructed by dividing it into two components: one derived from the conservation of elastic and kinetic energy, and the other representing the damping effects.

The first component of velocity $\dot{x}$ is calculated from the conservation of energy. During the rebound phase, the total energy consists of the elastic potential energy stored in the foam and the kinetic energy of the rebounding object:

$$E = \int_0^{x_{max}} kx^{\frac{3}{2}}dx = \frac{1}{2}mv_r^2 \quad (16)$$

From this, the maximum displacement x_{max} is expressed as:

$$x_{max} = \left(\frac{5}{4k}\cdot mv_r^2\right)^{\frac{2}{5}} \quad (17)$$

The relationship between v_r^2 and x_{max} follows as:

$$v_r^2 = \frac{4kx_{max}^{5/2}}{5m} \quad (18)$$

At any displacement, the velocity satisfies:

$$\int_0^x kx^{\frac{3}{2}}dx + \frac{1}{2}m\dot{x}^2 = \frac{1}{2}mv_r^2 \quad (19)$$

The first velocity component is then obtained:

$$\dot{x} = \sqrt{v_r^2 - \frac{4kx^{\frac{5}{2}}}{5m}} \quad (20)$$

The second component, attributed to damping effects, is assumed to vary approximately linearly with the displacement based on experimental results [2]:

$$\dot{x} = \left(\frac{x_{max}-x}{x_{max}}\right)(v_i - v_r) \quad (21)$$

Combining the elastic and damping components, the total velocity is given by:

$$\dot{x} = \sqrt{\frac{4kx_{max}^{5/2}}{5m} - \frac{4kx^{\frac{5}{2}}}{5m}} + \left(\frac{x_{max}-x}{x_{max}}\right)(v_i - v_r) \quad (22)$$

Substituting Eq. (22) into the energy balance Eq. (15) yields:

$$\frac{1}{2}mv_i^2(1 - C_r^2) = \int_0^{x_{max}} 2\zeta\sqrt{mk\sqrt{x}}\cdot\left(\sqrt{\frac{4kx_{max}^{5/2}}{5m} - \frac{4kx^{\frac{5}{2}}}{5m}} + \left(\frac{x_{max}-x}{x_{max}}\right)\cdot(v_i - v_r)\right)dx \quad (23)$$

Evaluating the integral and simplifying yields:

$$\frac{1}{2}mv_i^2(1 - C_r^2) = \frac{4\sqrt{5}\pi\zeta kx_{max}^{\frac{5}{2}}}{25} + \frac{32}{45}\zeta\sqrt{km}\cdot(v_i - v_r)x_{max}^{\frac{5}{4}} \quad (24)$$

From this, the damping ratio ζ is expressed as:

$$\zeta = \frac{9\sqrt{5}}{2}(1 - C_r^2)\cdot\frac{v_i^2}{9\pi v_r^2 + 16v_i v_r - 16v_r^2} \quad (25)$$

III. Experiment Evaluation of the Damping Performance of Foam

A. Test Rig Configuration

Based on the principles of hysteresis curves for elastic materials, it is possible to experimentally measure force and displacement data during the compression of foam by a piston. This data can then be used to directly calculate the damping loss factor. To facilitate this, a test rig was developed with a focus on cost-effectiveness, simplicity, stability, and high precision in measuring both indentation depth and force.

The test rig consists of several key components designed to work in unison. A motorized screw slide table drives the piston to compress the foam sample while enabling simultaneous collection of force and displacement data. The force sensor measures the force exerted during compression and is integrated into a groove at the top of the piston, which is specifically contoured to fit the sensor head. Displacement measurements are provided by a tie-rod displacement sensor, which is threaded to the piston and secured to a custom bracket for accurate alignment.

To ensure the system remains stable during operation, a metal base is used to secure the entire unit. An acrylic sample

container is employed to simulate real-world conditions by confining the foam sample, replicating the scenario of foam being enclosed within a cardboard box. This setup ensures that the experimental conditions closely mimic practical applications. The overall design of the test rig is illustrated in Fig. 1.

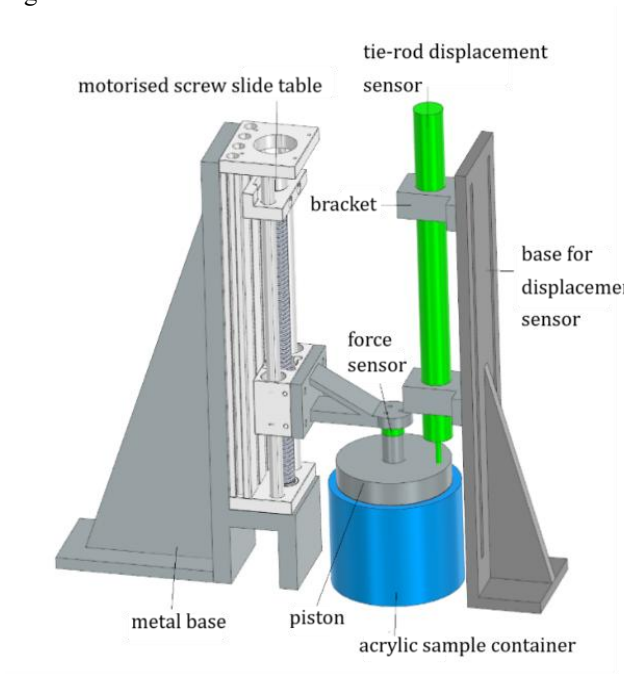

Fig. 1. Sketch of test configuration.

Although the controller of the motorized screw slide table can provide data about displacement, a separate displacement sensor is used to achieve higher measurement accuracy. The force and displacement data are collected and transmitted automatically and simultaneously, ensuring precise synchronization during operation. This design guarantees a reliable and repeatable experimental setup for the calculation of damping characteristics.

B. Results and Discussion

To investigate the effect of different samples on stiffness and damping characteristics, experiments were conducted using Expanded Polyethylene (EPE) foam with a standard sample diameter of 95 mm, a thickness of 40 mm, and a density of 15 kg/m³. This sample served as the baseline for subsequent experiments. The force-displacement graph for the different samples is presented in Fig. 2.

The stiffness-displacement relationships for the samples are shown in Fig. 3. The results indicate that the stiffness of all three samples decreases gradually during the compression phase, following a similar trend. From a microscopic perspective, this behavior is due to the open-cell structure of EPE foam, which absorbs and redistributes the applied force during initial compression. As compression progresses, the internal structure undergoes rearrangement, leading to localized stiffness reduction. This process is associated with the deformation and redistribution of the material's pore structure under stress.

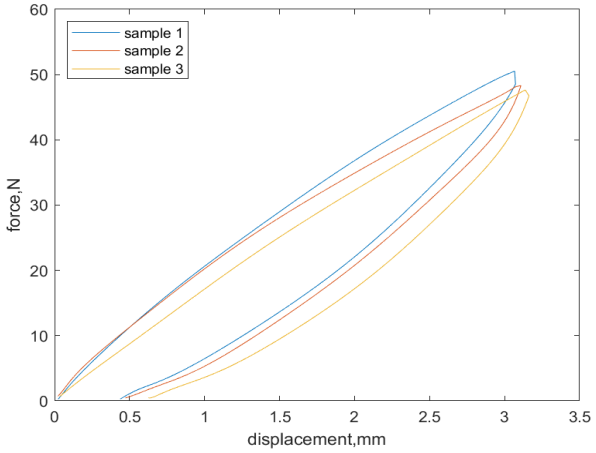

Fig. 2. Typical force-displacement curves for different samples.

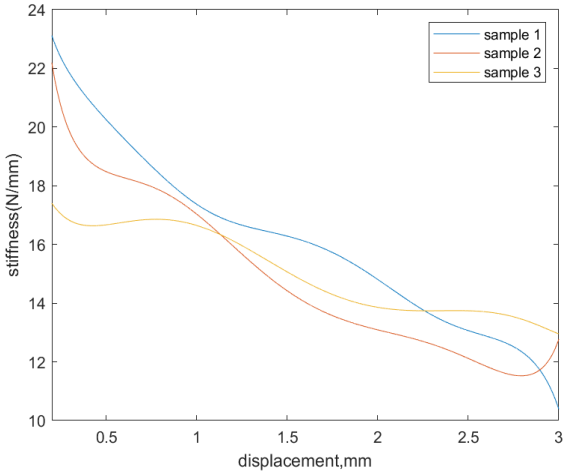

Fig. 3. Displacement dependent stiffness curves for different samples.

Permanent deformation of approximately 0.5 mm was observed for all samples. Slight differences in the compression ratios of the samples, approximately 0.3 mm, may be attributed to variations in thickness. Additionally, minor differences in stiffness are likely due to the glue adhesive layer, which exhibits uneven thickness across different sample positions. Variations in porosity, as samples were cut from different regions of the same plate, could also contribute to these discrepancies. Despite these factors, the dissipated energy and loss factors were consistent across the samples, as summarized in Table 1.

Table 1. Dissipated energy and loss factors for different samples

	Dissipated Energy (mJ)	Loss Factor
Sample1	34.76	0.4002
Sample2	33.59	0.4020
Sample3	34.41	0.4343

A separate experiment was conducted to examine the effects of repeated compression on a single EPE foam sample. The results showed a reduction in maximum displacement and an increase in stiffness after each compression cycle, along with a corresponding decrease in the dissipated energy and loss factor (see Table 2). After the third compression, permanent deformation stabilized, indicating the material had reached a new equilibrium state.

Table 2. Dissipated energy and loss factors for repeated compression of a single sample

	Dissipated energy (mJ)	Loss factor
First compression	34.76	0.4002
Second compression	30.01	0.3728
Third compression	28.53	0.3650

Microscopically, the observed behavior can be explained by the porous structure of the material. During the initial compression, internal gas and the polymer matrix experience significant stress, leading to large deformations. These include polymer chain rearrangement and gas compression, which result in permanent deformation upon unloading. After repeated compressions, the redistribution of internal gas and stabilization of polymer chains likely contribute to reduced deformation. These results demonstrate that reusing EPE foam leads to a reduction in damping capacity, though the decrease stabilizes after multiple uses.

The diameter, density, and thickness of packaging materials influence their mechanical properties and environmental performance. Optimizing these parameters reduces material usage and costs while enhancing sustainability. By studying the damping characteristics of materials with different thicknesses and densities, it is possible to identify configurations that minimize material consumption without sacrificing functionality.

The force-displacement and stiffness-displacement graphs for samples of varying thicknesses are shown in Figs. 4 and 5, respectively. The stiffness and corresponding Young's modulus are calculated from the force and geometrical data and summarized in Table 3.

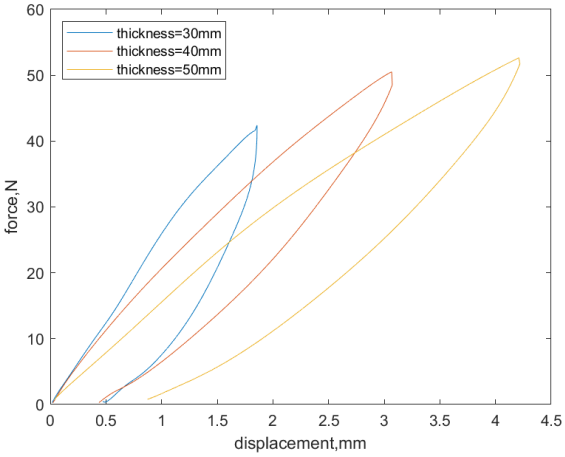

Fig. 4. displacement dependent force curves for test samples with respect to different thicknesses

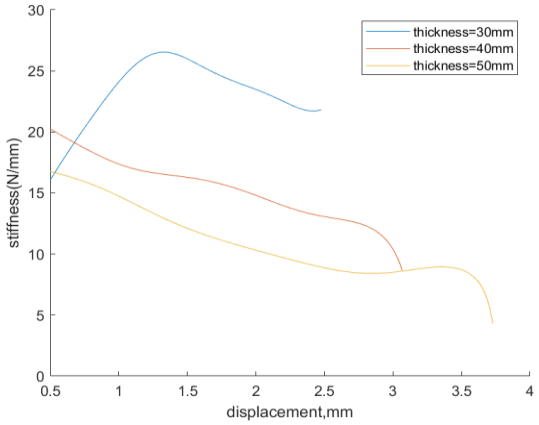

Fig. 5. displacement dependent stiffness curves for test samples with respect to different thicknesses.

Table 3. Dynamic properties for samples of different thicknesses

Thickness (mm)	Stiffness (N/mm)	Young's modulus (MPa)	Dissipated energy(mJ)	Loss factor
30	23.38	0.09895	18.92	0.3713
40	17.66	0.09966	34.25	0.4122
50	13.15	0.09275	46.10	0.4616

Both the dissipated energy and loss factor increase with thickness. This can be attributed to the presence of more pores and a more complex polymer chain structure, which increases resistance to energy transfer within the material.

Similarly, as for the diameter, dynamic properties of the foam with different diameter are provided in Table 4.

Table 4. Dynamic properties for samples of different diameters

Diameter (mm)	Stiffness (N/mm)	Young's modulus (MPa)	Dissipated energy(mJ)	Loss factor
35	1.882	0.07824	5.31	0.4242
65	8.891	0.1072	16.69	0.4320
95	17.66	0.09966	34.25	0.4122

The results suggest that Young's modulus is consistent for diameters of 65 mm and 95 mm, but it is lower at 35 mm, likely due to pre-compression caused by the piston's self-weight. The dissipated energy increases with diameter due to higher applied forces, but the loss factor remains consistent.

Dynamic properties with respect to the density are summarized in Table 5.

Table 5. Dynamic properties for samples of different density

Density(kg/m^3)	Dissipated energy (mJ)	Loss factor
15	34.25	0.4122
28	57.34	0.4395

Higher density leads to increased stiffness and dissipated energy, as the material absorbs more energy during compression. However, the loss factor remains nearly unchanged.

This section systematically analyzes the compression properties of EPE foam, as well as their effects on damping characteristics, laying a foundation for subsequent research. The study reveals that EPE foam is suitable for impact resistance and vibration damping applications, Furthermore, as the compression ratio increases, the loss factor of EPE foam decreases; as the compression speed increases, the loss factor initially rises and then stabilizes. In terms of material parameters, the loss factor of EPE foam is positively correlated with thickness, while density and diameter have no effect on the loss factor. Through an exploration of the mechanical behavior of these materials under different experimental conditions, we have gained a deeper understanding of the impact resistance for the foam.

IV. An Improved Model for Damping Obtained from Static Compression Experiments

In static compression experiments, we assume that the elastic force of EPE foam follows the Hertz contact model,

where the force is proportional to the 3/2 power of the displacement:

$$F = kx^{3/2} \tag{26}$$

This relationship is derived from the Hertz contact model, which describes the mechanical interaction between two elastic objects in contact, such as a sphere and a plane. The model assumes an infinitesimal initial contact area and stiffness. However, in this experiment, the contact surface between the piston and the EPE foam sample is flat, and the compression velocity is low, resulting in complete contact over the entire upper surface of the foam cylinder. This setup does not fully conform to the assumptions of the Hertz model.

To better describe the unloading behavior observed in the experiments, various functional forms were tested to fit the experimental data. The following quadratic function was found to provide a better fit:

$$F = ax^2 + bx \tag{27}$$

The fitted parameters are summarized in Table 6:

Table 6. fitting parameters of the load-deflection curve.

a($N \cdot mm^{-2}$)	3.30
b($N \cdot mm^{-1}$)	8.74
c($N \cdot mm^{-1.5}$)	11.03

Fig. 6 shows a comparison of the force-displacement graph for the experimental data and the fitted models.

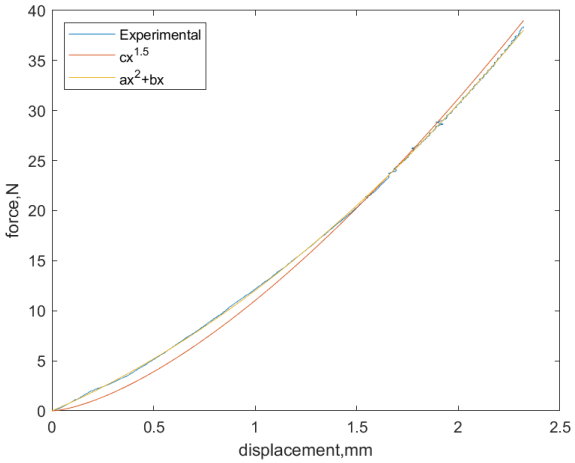

Fig. 6. Comparison of elasticity of the foam when subject to different ways of fitting.

The quadratic function in Eq. (27) achieves a much better fit, with a Root Mean Square Error (RMSE) less than one-tenth that of the Hertz model, as shown in Table 7.

Table 7. RMSE values when subject to different type of curve fitting

Fitting method	RMSE Value
$F = kx^{3/2}$	4.605e-3
$F = ax^2 + bx$	6.458e-4

The displacement-dependent stiffness becomes:

$$k(x) = ax + b \tag{28}$$

The natural frequency is then expressed as:

$$\omega_n(x) = \sqrt{\frac{ax+b}{m}} \tag{29}$$

The damping ratio can be expressed as:

$$\zeta = \frac{c(x)}{2\sqrt{m(ax+b)}} \tag{30}$$

Substituting these into the energy balance equation:

$$\frac{1}{2}mv_i^2(1 - C_r^2) = \int_0^{x_{max}} 2\zeta\sqrt{m(ax+b)}\dot{x} \cdot dx \tag{31}$$

Similarly, the conservation of energy equation becomes:

$$E = \int_0^{x_{max}} (ax + b)dx = \frac{1}{2}mv_r^2 \tag{32}$$

Solving for rebound velocity:

$$v_r^2 = \frac{\frac{2}{3}a{x_{max}}^3 + b{x_{max}}^2}{m} \tag{33}$$

The velocity at any displacement can then be calculated as:

$$\int_0^{x_{max}} (ax + b)dx + \frac{1}{2}m\dot{x}^2 = \frac{1}{2}mv_r^2 \tag{34}$$

Considering damping effects, the velocity can be expressed as:

$$\dot{x} = \sqrt{\frac{\frac{2}{3}a({x_{max}}^3 - x^3) + b({x_{max}}^2 - x^2)}{m}} + \left(\frac{x_{max} - x}{x_{max}}\right)(v_i - v_r) \tag{35}$$

The energy balance equation is rewritten as:

$$\frac{1}{2}mv_i^2(1 - C_r^2) = 2\zeta\sqrt{m}\int_0^{x_{max}} \sqrt{ax+b}\sqrt{\frac{\frac{2}{3}a({x_{max}}^3 - x^3) + b({x_{max}}^2 - x^2)}{m}}dx + 2\zeta\sqrt{m}\left(\frac{v_i - v_r}{x_{max}}\right)\int_0^{x_{max}} \sqrt{ax+b}(x_{max} - x)dx \tag{36}$$

Rearranging for the damping ratio, we have:

$$\zeta = \frac{1}{2}mv_i^2(1 - C_r^2)/\Big(2\sqrt{m}\int_0^{x_{max}} \sqrt{ax+b}\sqrt{\frac{\frac{2}{3}a({x_{max}}^3 - x^3) + b({x_{max}}^2 - x^2)}{m}}dx + \left(\frac{v_i - v_r}{x_{max}}\right)\int_0^{x_{max}} \sqrt{ax+b}(x_{max} - x)dx\Big) \tag{37}$$

The procedure to calculate impact damping ratio ζ from material hysteresis loop can be expressed as follows:

1. Convert the experimentally measured loss factor η into the coefficient of restitution, linking energy loss to rebound behavior.
2. Derive the rebound velocity based on maximum displacement.
3. Relate the impact velocity to rebound velocity and coefficient of restitution using:

$$v_i = \frac{v_r}{C_r} \tag{38}$$

4. Perform numerical integration for Eq. (37) using experimental fitting parameters and the mass of the sample.

A sensitivity analysis was conducted to evaluate the influence of mass on damping ratio, as shown in Fig. 7. The results indicate that the mass has minimal impact on the damping ratio calculation.

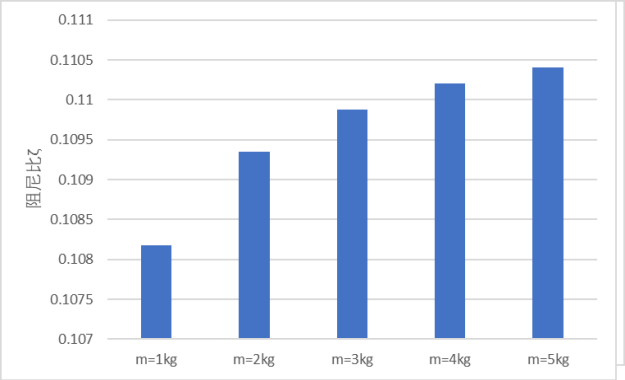

Fig. 7. Sensitivity analysis of mass on damping ratio.

In order to illustrate the calculation of the impact damping using static compression experimental data, a practical example is provided based on the parameters summarized in Table 8.

Table 8. Key Parameters for deriving the damping ratio

Parameter	Value	Units
a	3.30×10^{6}	Nm^{-2}
b	8.74×10^{3}	Nm^{-1}
x_{max}	0.0267	m
Compression Ratio	66.8	%
η	0.2324	—

Using the key parameters in Table 7 and substituting them into Eq. (37), the impact damping ratio derived from the static compression method is approximately:

$$\zeta\approx0.1099 \tag{39}$$

This example demonstrates the practical application of the proposed model for quantifying the damping properties of EPE foam. The approach highlights the effectiveness of static compression experiments in estimating damping ratios accurately, providing a reliable basis for material characterization and potential design optimizations.

V. Conclusion

This study conducted a comprehensive experimental and theoretical analysis of the damping characteristics of packaging filler materials. A custom-designed static compression experimental device was developed and employed to systematically test and analyze the damping properties of EPE pearl cotton. The study explored the influence of different sample conditions, experimental parameters, and material properties on the damping behavior. Based on experimental data fitting, a modified damping model was proposed, offering improved suitability for foam materials within specific ranges.

While the results of this study provide valuable insights, further testing is required to validate the refined model, particularly through impact testing, which could complement the findings from static compression experiments. Additionally, future research may explore alternative materials, such as air-filled bags and particulate fillers, whose damping characteristics are increasingly relevant in packaging applications. Investigating these materials may necessitate the development of new experimental methodologies to better capture their unique mechanical and damping behaviors.

This study lays a solid foundation for advancing the understanding of damping properties in packaging materials, with the potential for improving material selection and design in real-world applications.

Conflict of Interest

The author declares no conflict of interest.

References

[1] T. Feng *et al.*, "Experimental research of influences of foam material thickness on its stiffness and damping coefficient," *Packaging Engineering*, vol. 33, no. 9, 2012.

[2] C. Ge and B. Rice, "Impact damping ratio of a nonlinear viscoelastic foam," *Polymer Testing,* vol. 72, pp. 187–195, 2018.

[3] R. Jankowski, "Analytical expression between the impact damping ratio and the coefficient of restitution in the non-linear viscoelastic model of structural pounding," *Earthquake Engng Struct. Dyn.*, vol. 35, pp. 517–524, 2006.

[4] B. J. Ramirez and V. Gupta, "Energy absorption and low velocity impact response of open-cell polyurea foams," *Journal of Dynamic Behavior of Materials*, vol. 5, no. 2, pp. 132–142, 2019.

[5] K. L. Johnson, *Contact Mechanics*, Cambridge: Cambridge University Press, 1985.